

Chapter 4¹

Imaging Chambers for *Arabidopsis* Seedlings for Mitotic Studies² ³

Sidney L. Shaw, Mathew Siebe, and Timothy Cioffi⁴

Abstract⁵

Flowering plants evolved away from creating centrosomes or conventional microtubule organizing centers.⁶ Therein, plants have posed a long-standing challenge to many of the conventional ideas for mitotic spindle⁷ construction and the process of chromosome segregation. The *Arabidopsis* seedling has emerged as a⁸ leading model for plant cell biological studies of the cytoskeleton and vesicle trafficking. Here we describe⁹ methods for creating a reusable chamber for mitotic studies in both seedling root and shoot cells with¹⁰ instruction for best practices with conventional microscopic techniques.¹¹

Key words *Arabidopsis* mitosis, Kevin, Seedling imaging chamber¹²

1 Introduction¹³

The *Arabidopsis* seedling is a leading model system for studies of¹⁴ cell biological phenomena in flowering dicot plants. The genetic¹⁵ resources and small stature of the seedling provide advantages for¹⁶ studying a wide variety of cellular functions in the context of the¹⁷ developing organism. Developmental studies examining the timing¹⁸ and positions of cell division in the root and apical meristems have¹⁹ used both ad hoc and more formally engineered methods [1]²⁰ for identifying when and where cell division occurs [2, 3]. Cell²¹ biological explorations of mitosis, using high-resolution imaging²² techniques, have been less frequent in *Arabidopsis*, with more focus²³ on the later events related to the establishment and formation of²⁴ the cell division plane [4–6].²⁵

The fundamental mechanistic details of plant spindle formation²⁶ and chromosome segregation are not well explored and scarcely²⁷ appear in popular reviews of mitosis beyond the admission that²⁸ flowering plants do not have centrosomes or conventional micro-²⁹ tubule organizing centers [7–10]. Experiments performed in *Hae-*³⁰ *manthus* (tiger lily) endosperm cells [11, 12], *Tradescantia*³¹ (spiderwort) stamen hair cells [13], and *Nicotiana* (tobacco) cells³²

[14, 15] still constitute a large portion of the reviewed materials owing to their experimental accessibility for specific questions. Efforts in maize, a classic genetic system for plant studies, have focused more attention on meiotic processes than mitosis with a significant history developed around the control and function of centromeres [16, 17]. The development of liverwort and bryophyte (moss) systems, notably *Marchantia* and *Physcomitrella*, respectively, that feature both rapid molecular manipulation and highly predictable cell divisions has driven more direct study of the mitotic apparatus and the mechanics of chromosome segregation with a more conventional spindle architecture [10, 18–21]. Studies using *Arabidopsis* have appeared sporadically, with emphasis on signaling mechanisms surrounding the entrance to division, the positioning of microtubule nucleation complexes, and microtubule orientations in late telophase [4, 6, 8].

Several major factors impact the collection of high-resolution image data from flowering plants such as *Arabidopsis* [22, 23]. Most prominently, the plant cell wall is both highly refractive [24] and optically active in the rotation of polarized light. Most plant tissues also exhibit some level of autofluorescence across a broad spectrum of excitation and emission wavelengths. Finally, most plant cells undergoing mitosis are large enough that the nucleus or free chromosomes can move several microns within the axial focus of the microscope over a few seconds, requiring volume-based imaging methods. The combined effect is to make high-resolution (i.e., high numerical aperture) imaging a challenge from cell to cell [25]. Focusing through the cell wall, with refractive indexes varying between 1.39 and 1.45 and thickness varying over a wide range for different cell types, means that the exact focal point and quality of the diffraction-limited excitation or emission will change throughout the field. Moreover, the laser illumination from a point-scanning confocal microscope nearly always retains a high degree of polarization, a characteristic that can be reinforced or redirected as the light traverses the wall material to create a focal volume. The practical effect is that widefield fluorescence techniques and computational deconvolution rarely yield acceptable image data for analysis of live cells and confocal imaging often shows anomalous features in reconstructions of image stacks. The optical activity of the cell wall additionally hampers the application of super-resolution techniques that require polarized illumination to produce structured illumination [26].

The most successful high-resolution fluorescence methods for mitotic studies in flowering plants center on scanning confocal imaging techniques [23]. Chemically fixed specimens that have been immuno-labeled for molecules of interest and mounted in a medium that matches the expectations of current oil immersion lenses will provide the best resolution for light microscopy. For questions that can be approached with these methods, immunohistological techniques have been published that provide excellent

guidance for root and some leaf materials [27]. For live cell imaging, both point-scanning and spinning disk confocal microscopes have been successfully deployed for determining the spatial and temporal changes occurring during mitosis [6, 28]. The choice of technique often depends upon the tissue type, molecular probes, and specific questions being posed for the study. Light-sheet microscopy will add substantively to the repertoire of methods [29] available to plant cell biologists (cites) investigating mitotic events but has yet to appear in a viable commercial platform for high-resolution plant studies.

While the *Arabidopsis* epidermal hypocotyl cells have become a leading model for plant cytoskeletal biology, mitotic division in the hypocotyl is extremely rare. Therefore, proliferating epidermal cells (Fig. 1a) in the margins of the expanding cotyledon (embryonic leaf), the petiole (connects cotyledon to seedling), and the emerging apical meristem are targets for mitotic studies. Cells in these tissues do not undergo cell division in an entirely predictable manner, so holding seedlings in the dark until 2–6 h before imaging or selecting seedlings that are coming out of the dark phase of a diurnal light cycle can improve the chances of capturing cells going into mitosis. Cells from aerial parts of the seedling are robust to seedling manipulations such as mounting or drug treatment but are often difficult to position with respect to the optical pathway of the microscope.

Alternatively, epidermal root cells between the meristem and growth zone (Fig. 1b) undergo mitotic divisions with more regularity and typically divide along a predictable cell orientation. The *Arabidopsis* root is, however, delicate and prone to damage when taken off of solid growth medium for imaging in liquid media, often necessitating the use of special imaging chambers. Moreover, functional fluorescent tubulin probes have been difficult to create for the root, leading to a reliance on fluorescent MAPs for reporting the positions and dynamic properties of root microtubules [30].

To facilitate high-resolution live cell imaging of the plant root and cotyledon cells undergoing mitosis, we developed a relatively simple chamber for seedling germination that transfers directly and repeatedly between plant incubator and microscope stage (Fig. 1). The chamber may be constructed without special appliances or materials and serves to robustly handle seedlings through 6–10 days of growth.

2 Materials

1. Liquid medium: 0.5× Murashige and Skoog (MS) medium [31] using 2.2 g MS salts (Sigma-Aldrich) and 0.5 g MES buffer to 0.9 L of distilled water. Bring the media pH to 5.7 with KOH and the final volume to 1 L with distilled water.

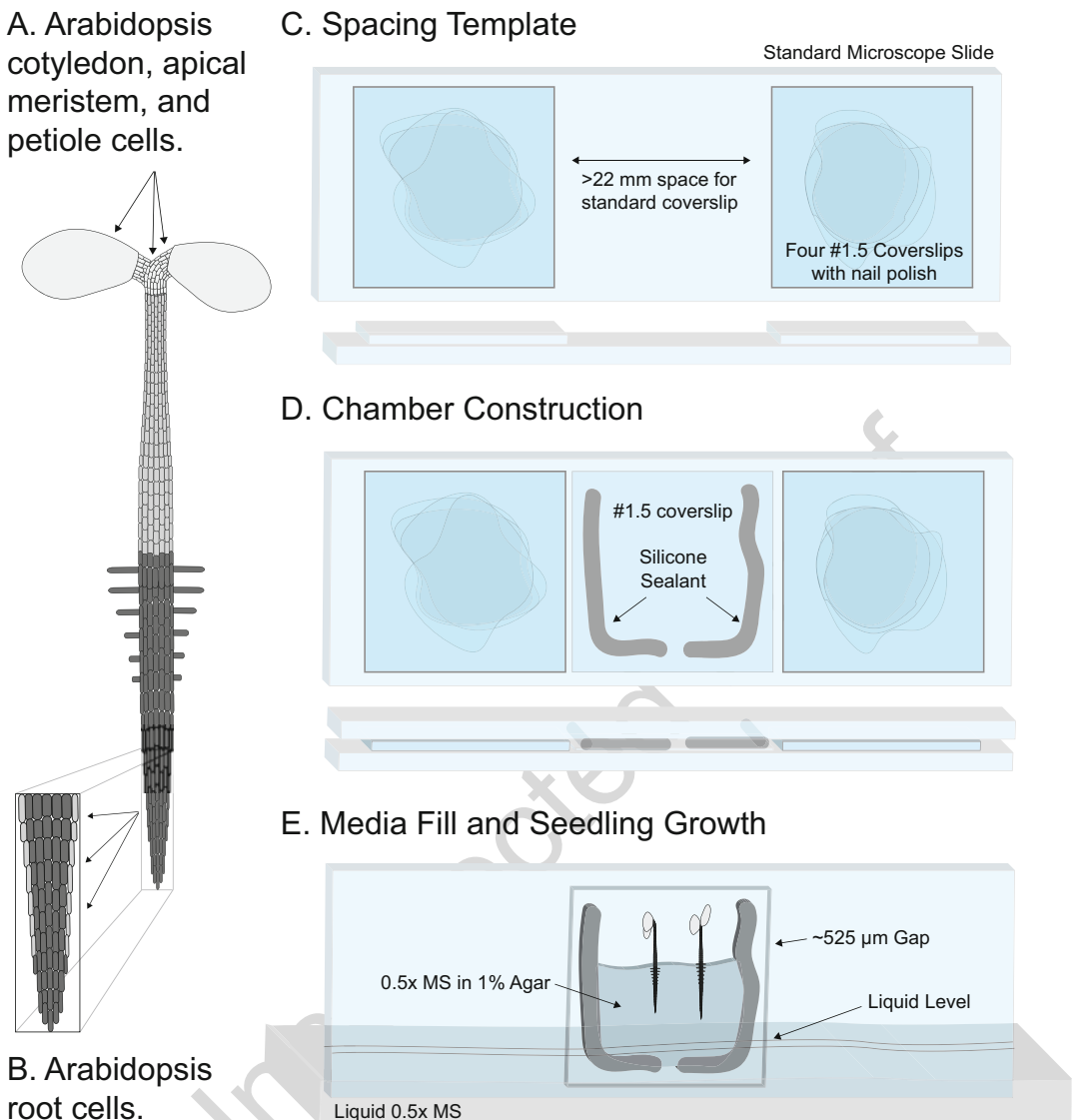


Fig. 1 Mitotic cells appear at the apical aerial portions (a) of the *Arabidopsis* seedling and in the beginning growth zone of the root tip (b). Imaging chamber is created by first making a spacing template (c) using stacks of four #1.5 coverslips adhered with nail polish. The chamber is constructed by placing a single #1.5 coverslip into the spacing template (d) and applying silicone sealant in a modified “U” pattern. A clean standard microscope slide is positioned on to the template creating a 525 μ m gap for seedling germination. The chamber is filled to half-capacity with agar plant media, and sterilized seed are placed into the chamber with the agar interface (e). Placing chambers vertically into a liquid allows seedling growth for 6–10 days

2. Solid medium: To create 1% w/v agar medium, use 10 g plant tissue culture grade agar (Sigma-Aldrich) per 1 L media and autoclave in bottles. 128
129
130
3. Aliquot hot liquid media to smaller (e.g., 250 mL) autoclaved bottles that can be warmed in a microwave or heat block to re-melt media at 95–98 °C before use in chambers. 131
132
133

4. Seed sterilization solution: Mix hydrogen peroxide and molecular biology grade ethanol in a 30/70 (v/v) ratio. Store at 4 °C in a sealed glass bottle covered with aluminum foil to protect from light. 134
135
136
137
5. Imaging chambers are made from standard (75 × 25 mm) glass microscope slides and #1.5 weight (22 × 22 mm) coverslips obtained from any of multiple sources. 138
139
140
6. Glass is pre-cleaned by submerging in 100% ethanol (v/v) and air-drying immediately prior to chamber construction. 141
142
7. Chambers are constructed using a marine-grade silicone-based adhesive and should be tested for shrinkage prior to use of chambers. Gorilla 100% Silicone Sealant (The Gorilla Glue Company, Cincinnati, OH, USA) is easily applied, cures in less than 60 min, holds glass well enough to reuse chambers, and shows an acceptably low level of contraction between glass slide and coverslip. 143
144
145
146
147
148
149

3 Methods

150

3.1 Imaging Chamber Spacer Template

The simple imaging chambers are created using a template to insure the correct spacing for seedling growth between the coverglass and slide. 151
152
153

1. Pre-clean one standard glass microscope slide and eight standard glass #1.5 weight coverslips by immersion in 100% ethanol and air-drying. 154
155
156
2. The spacing template (Fig. 1) uses two stacks of four coverslips held together by optical cement or nail polish. Wearing gloves to avoid transfer of oils or dust to each coverglass, use a small drop of nail polish to attach one coverslip to one end of the glass microscope slide. Attach a second coverglass to the microscope slide with nail polish at a position greater than 22 mm away, creating a gap for the placement of a coverslip during chamber construction. 157
158
159
160
161
162
163
164
3. Repeat the process of adding coverslips to both stacks, pressing down on each side gently to create a secure contact with no air gaps. Only a small drop of adhesive is required to hold the coverslips in place, and creating a uniformly aligned stack, where no coverslip is sticking out of the stack, will ease construction of imaging chambers. 165
166
167
168
169
170
4. Allow the reusable spacing template to cure until completely rigid (i.e., 1 h). Any optical cement or nail polish on the glass slide surface between coverslip stacks should be cleaned or removed with appropriate solvent (i.e., acetone). 171
172
173
174
175

3.2 Imaging Chamber Construction

The imaging chamber is constructed using a standard glass microscope slide and #1.5 (170 μm) thickness coverslip. The coverslip is affixed to the glass slide with a marine-grade silicon-based adhesive with relatively low form shrinkage.

1. Using forceps or gloves to prevent transfer of oils or dust, place a pre-cleaned #1.5 weight coverslip into the spacer template between the stacks of immobilized coverslips (Fig. 1). 180
181
182
2. Apply the silicone marine-grade sealant in a modified “U” shape around the periphery of the pre-cleaned coverslip, leaving a 1–2 mm gap at the base of the “U” shape (Fig. 1). The sealant should be applied in a careful bead to minimize the footprint and prevent closure of the gap in step 3. 183
184
185
186
187
3. Before the sealant has set, place a pre-cleaned standard glass microscope slide over the spacing template and in contact with the sealant (Fig. 1). Press the slide to insure that it is seated evenly on both stacks of affixed coverslips. 188
189
190
191
4. Allow the chamber to cure for 45–60 min in the spacer template before removing and use. If the sealant does not shrink, the chamber will have an internal gap of 520–550 μm , and the coverslip will remain entirely parallel to the microscope slide. 192
193
194
195
196
197

3.3 Preparing the Imaging Chamber

1. Warm the 1% agar plant media so that it is just melted using a microwave oven or heated water bath. 198
199
2. Optionally, we have sterilized chambers by submerging in ethanol and drying in a sterile hood prior to adding media. 200
201
3. Carefully hold the chamber or seat the chamber vertically on a folded piece of parafilm to prevent the liquid media from draining out of the gap in the bottom of the chamber. 202
203
204
4. Using a pre-heated 1 mL syringe or manual pipettor, carefully introduce 80–100 μL of the still liquid plant medium into the chamber and allow the media to solidify. The agar-based media should fill approximately 1/2 of the chamber volume and extend into the gap at the base of the chamber (Fig. 1). 205
206
207
208
209
5. The media in the chambers is highly susceptible to drying. We recommend using the chambers immediately. Chambers can be stored at 4 °C in a sealed container with a wet paper towel to prevent drying prior to use. 210
211
212
213
214

3.4 Seed Sterilization and Seedling Germination

1. We place 1–5 *Arabidopsis* seed on to a dry, creased filter paper in a tissue culture sterile hood. Up to 500 μL of sterilization solution is pipetted on to the seed and allowed to dry in the sterile hood. The sterilization reduces the impact of rapidly growing bacteria or fungi that can be carried with the harvested seed into the imaging chamber. 215
216
217
218
219
220

2. Seed are placed into the chamber resting on the agar interface 221 with the air. Seed are transferred using either a sterile tooth- 222 pick, wetted at the end to hold the seed, or the seed are gently 223 tapped into the chamber using the crease in the filter paper. 224
3. Chambers are placed in a sealed bag and placed in a small 225 lightproof box for storage at 4 °C for 24–48 h. The cold 226 treatment increases the synchrony of germination and early 227 growth. 228
4. After cold treatment, the chamber is set upright into a recycled 229 microscope slide box or other container where the open space 230 at the bottom of the chamber can be placed in contact with 231 water or media in the bottom of the container (Fig. 1e). Wick- 232 ing of the liquid through the open space in the bottom of the 233 slide into the agar media will prevent the media from drying 234 and provide a constant level of hydration for the seedling(s). 235 The chamber and container are kept in a transparent bag to 236 prevent the liquid in the container from drying out or concen- 237 trating due to evaporation. 238
5. Imaging chambers are moved to plant incubators for germina- 239 tion and growth under light regimes and temperatures that are 240 commensurate with the experimental goals. For imaging the 241 growing root tip, the chambers are tilted ~10° from vertical so 242 that the root tips will grow against the coverslip surface. 243
6. For continuous dark growth, chambers containing seed taken 244 from the 4 °C cold treatment are placed in the incubator under 245 lighted conditions for 1–4 h prior to being placed into a 246 lighttight container. The light treatment, together with the 247 change in temperature, results in more consistent germination 248 times. 249
7. The chambers are kept for as long as 6 days for continuous 250 dark-grown, and for 10 days, for light-grown and light-cycled 251 seedlings. 252

3.5 Imaging Fluorescent Histone H2B Plant Lines in Root Cells

Identifying pre-mitotic cells for imaging in animal systems is greatly 254 facilitated by changes in cell morphology and adhesion (e.g., 255 rounding up) during late S-phase and G2. Plant cells have no 256 correlate changes in cell shape and do not typically undergo divi- 257 sions in clear temporal progressions. Several FUCCI-related mar- 258 kers have been used to indicate when plant cells have entered 259 S-phase [32], though many S-phase cells in plant tissues do not 260 progress through to mitosis, opting for endoreduplication. There- 261 fore, we have used a histone H2B fluorescent protein fusion as a 262 marker for finding prometaphase cells prior to nuclear envelope 263 breakdown and spindle formation (Fig. 2). 264

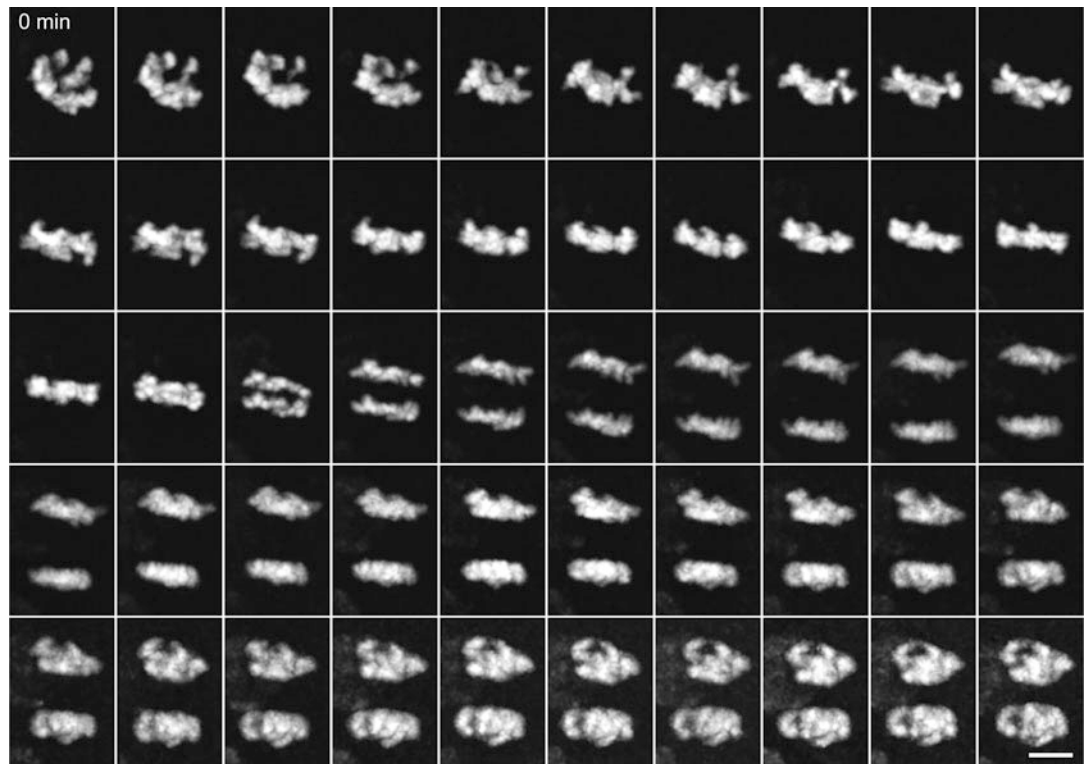


Fig. 2 Spinning disk confocal microscopy of mCherry-H2B imaged in *Arabidopsis thaliana* root cell undergoing mitosis. Time-lapsed images taken at 1.5 min intervals created from 40 frame Z-series (0.2 μ m steps) arranged in rows from left to right. A 60 \times silicone oil immersion objective was used with 80 ms exposures on an Olympus OSR spinning disk confocal microscope using a Hamamatsu sCMOS V3.2 camera. The 50-frame series shows chromosomes just at nuclear envelope breakdown followed by congression to the metaphase plate, anaphase, and the decondensation of the chromatin during nuclear reformation. Scale bar = 5 μ m

1. Growing root tips expressing an mCherry-histone H2B fusion protein under the control of a constitutive CaMV35S promoter (courtesy of Mark Estelle) show changes in nuclear morphology prior to mitosis. 265
266
267
268
2. Take the chamber out of the incubator and gently dry the coverslip face with a lens-cleaning tissue. 269
270
3. For live cell imaging, the refractive index changes as light passes through the coverslip and into the root are best matched by water immersion, silicone oil immersion, or glycerol immersion objective lenses with effective numerical apertures from 1.1 to 1.31. Conventional oil immersion objectives, with a numerical aperture above 1.3, will show rapidly increasing aberration when focusing beyond the first 10 μ m from the coverslip surface. 271
272
273
274
275
276
277
278

4. If at all possible, choosing an objective lens with a rotating correction collar will greatly improve the achievable contrast for the specimen. Adjusting the collar to find the brightest possible image at a depth that is midway through a prescribed specimen will suffice for live cell imaging purposes. 279
280
281
282
283
5. Mitotic progression occurs over a 10–15 time course in wild-type *Arabidopsis* root cells where the choice of image acquisition time, number of images in an axial stack, and time interval between frames will depend upon the experimental goals. 284
285
286
287
6. Note that most nuclei in epidermal cells appear at the far side of the cell and complete mitosis in a position that depends upon cell geometry. The post-mitotic formation of the cell wall tends to attach at the far side of the cell and proceed bidirectionally toward the outer face of the cell, necessitating a volume-based imaging approach for capturing key events through the process. 288
289
290
291
292
293
294
7. Note that most common lines expressing a fluorescent protein fused to alpha or beta tubulin do not show enough incorporation of the probe in root cells for imaging microtubules directly. Probes such as End Binding 1 (EB1b-GFP; cite) and a microtubule binding domain taken from animal cells (MBD-GFP; cites) have some use for mitotic studies in root cells. 295
296
297
298
299
300
301
302

3.6 Imaging Mitosis in Seedling Cotyledon and Apical Meristem

The appearance of mitotic figures in the accessible aerial portions of the seedling is less predictable than in the growing root tips. Keeping seedlings in the dark until 1–3 h prior to imaging will induce the cotyledons to undergo significant developmental changes related to de-etiolation. Those changes will include cell divisions in some marginal cells where the distance between coverslip and mitotic spindle can be minimized (Fig. 3). 303
304
305
306
307
308
309

Increased frequencies of division are also observed when seedlings are coming out of the first day-night light cycle. Tilting the chambers 10° in the direction of the microscope slide will improve the chances of having cells in the cotyledon or apical meristem close to the coverslip. 310
311
312
313
314

1. To accommodate high-numerical aperture lenses, fill the upper portion of the chamber with sterilized tap water or plant media at least 30 min prior to imaging. This can include pharmacological treatments, live cell stains, or other experimental treatments. Neat distilled water is not recommended as it will osmotically shock the plant requiring a longer recovery time. 315
316
317
318
319
320
2. Identify cells that are as close to the coverslip surface as possible to improve the fidelity of the imaging light path. Positioning mitotic cells close to the coverslip for live cell imaging is made difficult by the shape of the organs, often necessitating longer working distance objective lenses with lower working 321
322
323
324
325

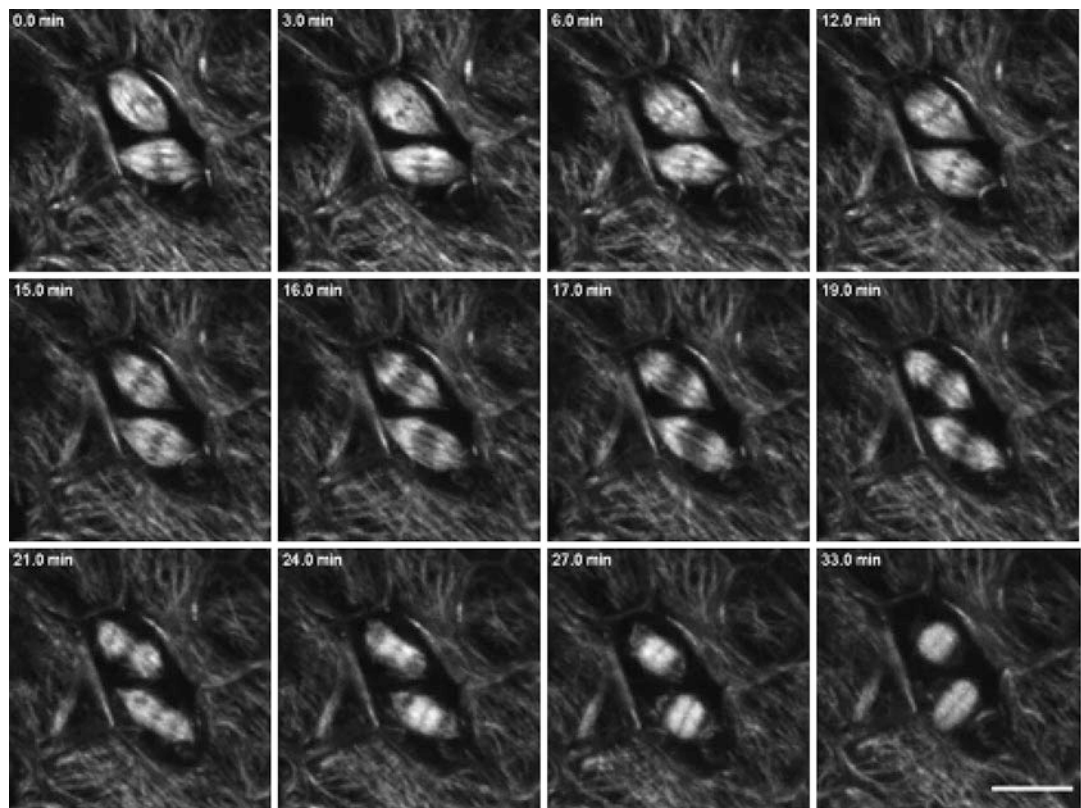


Fig. 3 Selected time points from spinning disk microscopy of *Eb1b-GFP* imaged in *Arabidopsis thaliana* cotyledon epidermal cells undergoing mitosis. Time-lapsed images of two adjacent cells made from 40-frame Z-series (0.2 μ m steps) arranged in rows from left to right. A 60 \times silicone oil immersion objective was used with 80 ms exposures on an Olympus OSR spinning disk confocal microscope using a Hamamatsu sCMOS V3.2 camera. Series includes mitotic congression to the metaphase plate, anaphase, and the formation of the plant phragmoplast array associated with formation of the new cell wall. Scale bar = 5 μ m

numerical apertures. In this circumstance, conventional oil immersion objective lenses perform substantially worse than water, silicone oil, or glycerol immersion objective lenses owing to the spherical aberration. Multi-color imaging suffers dramatically for both axial and lateral colocalization.

3. Using a spinning disk or point-scanning confocal microscope will provide a starting point for gaining contrast in the cotyledon or early apical meristem. Because of the autofluorescence in these aerial tissues, we image control plants, not expressing fluorescent proteins, to determine the degree to which the autofluorescence is contributing to the final image. Highly structured autofluorescence (e.g., background shapes) or a standard deviation of the local mean values more than 10–15% of the expected signal from the fluorescent proteins should initiate a search for more restrictive band-pass filters or using different fluorescent probes.

326

327

328

329

330

331

332

333

334

335

336

337

338

339

340

341

4. Mitotic progression in the aerial parts of the seedling occurs 342
over a 15–25 time course in wild-type *Arabidopsis* where the 343
choice of image acquisition time, number of images in an axial 344
stack, and time interval between frames will depend upon the 345
experimental goals. 346

347

3.7 Alternative Imaging Methods

Techniques other than confocal microscopy can be used successfully to image mitosis in *Arabidopsis* seedlings but require a higher level of familiarity with both the instrumentation and the specific cell types. Conventional widefield fluorescence imaging of living specimens rarely produces useful data because the out-of-focus fluorescence from the mitotic spindle typically overwhelms the in-focus image. Computational image deconvolution of widefield fluorescence images also fails under most circumstances because of the inhomogeneous optical aberrations introduced by the cell wall material. Multi-photon imaging in plant systems offers the advantage of imaging deeper and with potentially less overall photodamage to the cells when compared to confocal imaging [33]. However, the loss of lateral resolution, owing to the longer wavelength excitation, and the difficulty in controlling the excitation energy through depth make this technique challenging. Super-resolution STED techniques have shown very limited success in plant systems, with newer time-gated systems providing information for cortical structures [34]. Light-sheet microscopy offers a much gentler means of extracting fluorescent signals and should be markedly faster than point-scanning confocal microscopy [29]. The convex shape of the plant and the optical properties of the plant cell wall make current light-sheet microscopes difficult to apply for mitotic studies where shading and distortions often preclude collection of data. Newer light-sheet imaging designs with numerical apertures closer to 1.33 will likely improve the use of this technology dramatically. Total internal reflectance (TIRF) is not an appropriate choice for mitotic studies because the depth of field and position of the mitotic spindle with reference to the coverslip surface extend well beyond the evanescent field generated under nearly all circumstances. Related techniques have been very successful for imaging cortical structures when cells are appressed to the coverslip [35].

For bright-field imaging of mitosis in plant cells, phase-contrast microscopy does not have the same utility as it does for animal cells because the cell wall accentuates the phase differences in the light path, increasing the flare or optical ringing in the image. Differential interference contrast (DIC) imaging works surprisingly well for visualizing the segregation of chromosomes where a monochromatic illumination filter is strongly encouraged (e.g., the green filter in some widefield light paths) to limit dispersion that will reduce contrast in the image.

389

4 Notes

390

1. The largest microscope-independent factor impacting data quality is the position of the cell relative to the objective lens front element. The closer the mitotic cell is to the lens, the better the signal collection. Moreover, keeping the outer (periclinal) cell wall perpendicular to the optical axis, rather than at an angle, reduces the negative optical effects introduced by the cell wall materials. 391
392
393
394
395
396
397
2. Because these plant tissues do not undergo a synchronous or well-predicted temporal pattern of cell divisions, using a light regime to improve the probability of finding cells going into mitosis markedly increases the likelihood of success. 398
399
400
401
3. Water, glycerol, and silicone oil immersion objective lenses provide consistently better three-dimensional image volumes than conventional oil immersion objective lenses. For specimens in these chambers, a numerical aperture above 1.35 will produce more aberrations, degrading the final image, than lenses designed to work with water-based media. Water immersion objectives are significantly more sensitive to coverslip flatness in the optical path requiring careful mounting of the coverslip with spacers when using this chamber system. 402
403
404
405
406
407
408
409
410

412 References

1. Grossmann G, Guo WJ, Ehrhardt DW et al (2011) The RootChip: an integrated microfluidic chip for plant science. *Plant Cell* 23: 4234–4240
2. Rahni R, Birnbaum KD (2019) Week-long imaging of cell divisions in the *Arabidopsis* root meristem. *Plant Methods* 15:30
3. Shapiro BE, Tobin C, Mjolsness E et al (2015) Analysis of cell division patterns in the *Arabidopsis* shoot apical meristem. *Proc Natl Acad Sci U S A* 112(15):4815–4820
4. Miao H, Guo R, Chen J et al (2019) The gamma-tubulin complex protein GCP6 is crucial for spindle morphogenesis but not essential for microtubule reorganization in *Arabidopsis*. *Proc Natl Acad Sci U S A* 116(52): 27115–27123
5. Mravec J, Petrasek J, Li N et al (2011) Cell plate restricted association of DRP1A and PIN proteins is required for cell polarity establishment in *Arabidopsis*. *Curr Biol* 21(12): 1055–1060
6. Murata T, Sano T, Sasabe M et al (2013) Mechanism of microtubule array expansion in the cytokinetic phragmoplast. *Nat Commun* 4: 1967
7. Baskin TI, Cande WZ (1990) The structure and function of the mitotic spindle in flowering plants. *Annu Rev Plant Physiol Plant Mol Biol* 41(1):277–315
8. Lee YJ, Liu B (2019) Microtubule nucleation for the assembly of acentrosomal microtubule arrays in plant cells. *New Phytol* 222(4): 1705–1718
9. Wadsworth P, Lee WL, Murata T et al (2011) Variations on theme: spindle assembly in diverse cells. *Protoplasma* 248(3):439–446
10. Yamada M, Goshima G (2017) Mitotic spindle assembly in land plants: molecules and mechanisms. *Biology* 6(1):6
11. Euteneuer U, Jackson WT, McIntosh JR (1982) Polarity of spindle microtubules in *Haemanthus* endosperm. *J Cell Biol* 94(3): 644–653
12. Smirnova EA, Bajer AS (1994) Microtubule converging centers and reorganization of the interphase cytoskeleton and the mitotic spindle in higher plant *Haemanthus*. *Cell Motil Cytoskeleton* 27(3):219–233
13. Wolniak SM, Larsen PM (1992) Changes in the metaphase transit times and the pattern of

465 sister chromatid separation in stamen hair cells 511
466 of *Tradescantia* after treatment with protein 512
467 phosphatase inhibitors. *J Cell Sci* 102(Pt 4): 513
468 691–715 514
469 14. Cronshaw J, Esau K (1968) Cell division in 515
470 leaves of *Nicotiana*. *Protoplasma* 65(1):1–24 516
471 15. Xu J, Lee YJ, Liu B (2020) Establishment of a 517
472 mitotic model system by transient expression of 518
473 the D-type cyclin in differentiated leaf cells of 519
474 tobacco (*Nicotiana benthamiana*). *New Phytol* 520
475 226(4):1213–1220 521
476 16. Dawe RK, Lowry EG, Gent JI et al (2018) A 522
477 kinesin-14 motor activates neocentromeres to 523
478 promote meiotic drive in maize. *Cell* 173(4): 524
479 839–850.e18 525
480 17. Rhoades MM (1950) Meiosis in maize. *J 526
481 Hered* 41(3):59–67 527
482 18. Brown RC, Lemmon BE (2011) Dividing 528
483 without centrioles: innovative plant microtubule 529
484 organizing centres organize mitotic spindles in 530
485 bryophytes, the earliest extant lineages of land 531
486 plants. *AoB Plants* 2011:plr028 532
487 19. Brown RC, Lemmon BE, Horio T (2004) 533
488 Gamma-tubulin localization changes from 534
489 discrete polar organizers to anastral spindles and 535
490 phragmoplasts in mitosis of *Marchantia polymorpha* L. 536
491 *Protoplasma* 224(3–4):187–193 537
492 20. Buschmann H, Holtmannspotter M, Borchers 538
493 A et al (2016) Microtubule dynamics of the 539
494 centrosome-like polar organizers from the 540
495 basal land plant *Marchantia polymorpha*. *New 541
496 Phytol* 209(3):999–1013 542
497 21. Hiwatashi Y, Obara M, Sato Y et al (2008) 543
498 Kinesins are indispensable for interdigititation 544
499 of phragmoplast microtubules in the moss 545
500 *Physcomitrella patens*. *Plant Cell* 20(11): 546
501 3094–3106 547
502 22. Fricker M, Runions J, Moore I (2006) Quantitative 548
503 fluorescence microscopy: from art to science. *Annu Rev Plant Biol* 57:79–107 549
504 23. Shaw SL, Ehrhardt DW (2013) Smaller, faster, 550
505 brighter: advances in optical imaging of living 551
506 plant cells. *Annu Rev Plant Biol* 64:351–375 552
507 24. Vogelmann TC (1993) Plant-Tissue Optics. 553
508 *Annu Rev Plant Physiol Plant Mol Biol* 44: 231–251

25. Shaw SL (2006) Imaging the live plant cell. *Plant J* 45(4):573–598
26. Shaw SL, Thoms D, Powers J (2019) Structured illumination approaches for super-resolution in plant cells. *Microscopy* 68(1): 37–44
27. Celler K, Fujita M, Kawamura E et al (2016) Microtubules in plant cells: strategies and methods for immunofluorescence, transmission electron microscopy, and live cell imaging. *Methods Mol Biol* 1365:155–184
28. Vos JW, Pieuchot L, Evrard JL et al (2008) The plant TPX2 protein regulates prospindle assembly before nuclear envelope breakdown. *Plant Cell* 20(10):2783–2797
29. Maizel A, von Wangenheim D, Federici F et al (2011) High-resolution live imaging of plant growth in near physiological bright conditions using light sheet fluorescence microscopy. *Plant J* 68(2):377–385
30. Marc J, Granger CL, Brincat J et al (1998) A GFP-MAP4 reporter gene for visualizing cortical microtubule rearrangements in living epidermal cells. *Plant Cell* 10(11):1927–1940
31. Murashige T, Skoog F (1962) A revised medium for rapid growth and bio assays with tobacco tissue cultures. *Physiol Plant* 15(3): 473–497
32. Yin K, Ueda M, Takagi H et al (2014) A dual-color marker system for *in vivo* visualization of cell cycle progression in *Arabidopsis*. *Plant J* 80(3):541–552
33. Feijó JA, Moreno N (2004) Imaging plant cells by two-photon excitation. *Protoplasma* 223(1):1–32
34. Molines AT, Marion J, Chabout S et al (2018) EB1 contributes to microtubule bundling and organization, along with root growth, in *Arabidopsis thaliana*. *Biol Open* 7(8):bio030510
35. Konopka CA, Bednarek SY (2008) Variable-angle epifluorescence microscopy: a new way to look at protein dynamics in the plant cell cortex. *Plant J* 53(1):186–196